

\mathcal{PT} symmetry with a system of three-level atoms

Chao Hang¹, Guoxiang Huang¹, and Vladimir V. Konotop²

¹ *State Key Laboratory of Precision Spectroscopy and Department of Physics, East China Normal University, Shanghai 200062, China*

² *Centro de Física Teórica e Computacional and Departamento de Física, Faculdade de Ciências, Universidade de Lisboa, Avenida Professor Gama Pinto 2, Lisboa 1649-003, Portugal*

We show that a vapor of multilevel atoms driven by far-off resonant laser beams, with possibility of interference of two Raman resonances, is highly efficient for creating parity-time (\mathcal{PT}) symmetric profiles of the probe-field refractive index, whose real part is symmetric and imaginary part is anti-symmetric in space. The spatial modulation of the susceptibility is achieved by proper combination of standing-wave strong control fields and of Stark shifts induced by a far-off-resonance laser field. As particular examples we explore a mixture of isotopes of Rubidium atoms and design a \mathcal{PT} -symmetric lattice and a parabolic refractive index with a linear imaginary part.

PACS numbers: 42.50.Gy, 42.65.An, 11.30.Er

While non-Hermitian operators obeying pure real spectra, like for example the Bogoliubov-de Gennes [1] spectral problem, linear stability problem for nonlinear waves, or simply a parabolic potential with linear imaginary part [2], are known in physics for long time, it was only due to the work [3] that fundamental importance of such operators became widely recognized. It was discovered in [3] that there exists a wide class of complex potentials of Schrödinger equation obeying pure real spectra, and even most importantly, that this property is intrinsically related to the parity (\mathcal{P}) and time (\mathcal{T}) symmetries of physical systems. This discovery triggered the discussion [4] on the fundamentals of quantum mechanics whose axioms are based on Hermitian operators for observables. Further growth of interest in the theory of parity-time (\mathcal{PT}) symmetric potentials was originated by suggestions of implementation of \mathcal{PT} symmetry in a waveguide with gain and absorption [5], which was based on the analogy between quantum mechanics and paraxial optics where the refractive index plays the role of the potential in the Schrödinger equation. In optics \mathcal{PT} -symmetric refractive index profiles (i.e. obeying gain and losses of a given geometry) has been experimentally realized using process of four-wave mixing in Fe-doped LiNbO₃ substrate [6]. The possibility of optical realization of \mathcal{PT} symmetric potentials motivated various suggestions of practical applications, like nonreciprocal wave propagation [6, 7], implementation of coherent perfect absorber [8], giant wave amplification [9], etc. Experimental realization of \mathcal{PT} -symmetry using plasmonics [10] and temporal simulation of lattices using optical couplers [11] were also reported.

In this Letter we demonstrate the possibility of practical implementation of spatially distributed \mathcal{PT} -symmetric refractive index, i.e. the one having the property $n(x) = n^*(-x)$, in vapors of multi-level atoms driven by control fields with properly chosen Raman resonances and by a far-off-resonant Stark field.

First we recall some recent achievements in creation of large susceptibilities in atomic vapors controlled by ex-

ternal laser beams. While such systems are intrinsically dissipative, it was suggested in [12] and shown experimentally in [13], that using the destructive interference in imaginary part of susceptibility, it is possible to achieve large real refractive indexes keeping the absorption small enough. Recently, the idea of using two far-off-resonant control fields for realizing high susceptibility with nearly zero absorption of a probe field was developed theoretically [14] and confirmed experimentally [15]. An alternative way of achieving similar effect was proposed in [16] where two Λ -systems were explored in order to excite two Raman resonances (see also Ref. [17]).

Since the above mentioned schemes use the interference of two Raman resonances, one of which resulting in gain and another in absorption, the imaginary part of probe-field susceptibility appears as a non-monotonic function of the frequency with both positive (gain) and negative (absorbing) domains. Even more remarkable property is the possibility to design distributions where real and imaginary parts of the susceptibility appear respectively as even and odd functions of the probe-field frequency [14–17]. Since for a monochromatic beam the change $\omega \rightarrow -\omega$ is equivalent to the change $t \rightarrow -t$ the last property can be viewed as a time inversion symmetry. Thus our goal can be formulated as completing this time symmetry by the symmetry in the coordinate space.

To achieve this goal we choose the scheme based on mixture of two species of Λ -atoms, similar to the one explored in [16]. The involved atomic states will be assigned as $|g, s\rangle$ (ground state), $|a, s\rangle$ (lower state), and $|e, s\rangle$ (excited state), hereafter $s = 1, 2$ indicates the specie of the atoms (Fig. 1). The species have atomic densities N_1 and N_2 , respectively ($N = N_1 + N_2$ being total atomic density). Ω_p is the half Rabi frequency of the probe field coupling $|g, s\rangle \leftrightarrow |e, s\rangle$ and $\Omega_{1,2}$ are half Rabi frequencies of two control fields coupling $|a, s\rangle \leftrightarrow |e, s\rangle$. All fields are far-off resonant, which is guaranteed by condition $\Delta_s \gg \Omega_s$, where $\Delta_s = \omega_{e,s} - \omega_{a,s} - \omega_c$ is one-photon detuning with $\hbar\omega_{l,s}$ ($l = g, a, e$) being the eigen energy

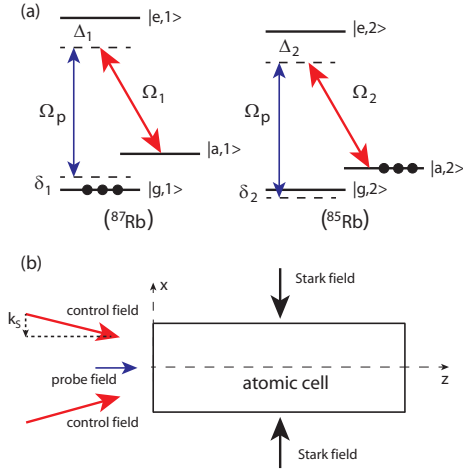


FIG. 1: (color online) (a) Two Λ -systems and Raman transitions used for obtaining \mathcal{PT} -symmetric refractive index. Initially populated levels are indicated by the filled circles. (b) Possible geometry for the suggested scheme. All notations are defined in the text.

of the state $|l, s\rangle$, and ω_p (ω_c) being the center frequency of the probe (coupling) field. Notice that one can explore different cases by changing signs of the two-photon detuning, defined by $\delta_s = \omega_{a,s} - \omega_{g,s} - (\omega_p - \omega_c)$. In Fig. 1(a) we show an example of the proposed scheme where $\delta_1 > 0$ and $\delta_2 < 0$, what corresponds to the \mathcal{PT} symmetric lattice obtained below. In our configuration, the first scheme ($s = 1$) exhibits two-photon absorption for the probe field while the second one ($s = 2$) provides two-photon gain.

Spatial modulation of the probe-field susceptibility can be achieved by using x -dependent control-field [with Rabi frequency $\Omega_s(x)$]. Such field, however affects both one- and two-photon detunings. Therefore we explore the second possibility, which is modulation of relative energy-level shifts along x -direction resulting in the dependence $\Delta_s = \Delta_s(x)$. This task can be achieved if a strong, far-detuned laser field $E_S(x) \cos(\omega_S t)$, where E_S and ω_S are respectively amplitude and frequency, is applied to the system. This field originates Stark shifts of levels by $\Delta E_{S,s}(x) = -\frac{1}{4}\alpha_{l,s}E_S^2(x)$, where $\alpha_{l,s}$ is the scalar polarizability of the level $|l, s\rangle$. Below $E_S(x)$ is referred to as the Stark field. If within the required accuracy one can consider $\alpha_{g,s} \approx \alpha_{a,s}$, i.e. the difference of Stark shifts between the ground-state sublevels is negligible (this is the situation we consider below). Then δ_s is not affected by the Stark field, while for the one-photon detunings we have $\Delta_s(x) = \Delta_s - (\alpha_{e,s} - \alpha_{g,s})E_S^2(x)/(4\hbar)$. Thus the Stark field allows one to manipulate the spatial distribution of $\Delta_s(x)$, on the one hand, and on the other hand being far-off-resonant does not lead to power broadening of lines due to low rate of transitions [18].

Since the Stark shift usually appears in the second order of the perturbation theory, it requires relatively

strong electric fields. Taking into account the characteristics of the available lasers, this may impose strong limitations, because the characteristic scale of the spatial modulation of $\Delta_s(x)$ is of order of the wavelength of the Stark field λ_S . For the typical order of the control field amplitudes $E_c \sim 10^2$ V/cm ($\Omega_{1,2} \sim 2\pi \times 514$ MHz), the required amplitude of the Stark field must be three orders of magnitude larger, i.e. $E_S \sim 10^5$ V/cm (for more detail estimates see below). Being focused into a spot of a diameter of ≈ 30 μm this requires laser powers of order of 100 W. Nowadays such powers can be achieved using say quantum cascade lasers [19, 20] operating at micron wavelengths (in [19] it was $\lambda_S = 4.45$ μm , which will be used in our estimates).

For the described model the susceptibility of the probe field can be computed from the density-matrix formalism within the rotating-wave approximation. Its functional form is the same as in [16] with the difference that now the two-photon detuning and control field depend on the spatial coordinate:

$$\frac{\chi_p(x)}{\chi_0} = \frac{\delta_1 - i\gamma_{ag}}{(\delta_1 + \Delta_1(x) - i\gamma_{eg})(\delta_1 - i\gamma_{ag}) - |\Omega_1(x)|^2} - \eta \frac{|\Omega_2|^2(\Delta_2(x) + i\gamma_{ag})^{-1}}{(\delta_2 + \Delta_2(x) - i\gamma_{eg})(\delta_2 - i\gamma_{ag}) - |\Omega_2(x)|^2}. \quad (1)$$

Here $\chi_0 = N_1 d_{eg,1}^2 / (\varepsilon_0 \hbar)$, ε_0 is the vacuum permittivity, $\eta = N_2 d_{eg,2}^2 / N_1 d_{eg,1}^2$ characterizing the ratio between the specie densities is considered as a free parameter, the $d_{...s}$ stands for the dipole moment of the transition between the ground and excited states of the s -the system.

Notice that generally speaking in a warm vapor large Doppler broadened line widths (typically $\Delta\omega/\omega \sim 10^{-6}$ [18]) may degrade the effectiveness of resonant schemes. While in our case such broadening would not be important for large one-photon detuning it is of order of the two-photon detuning. It turns out, however, that the effect of this line broadening can be significantly suppressed (by the factor $|\omega_c - \omega_p|/\omega_c$) if far-off-resonant co-propagating beams (see e.g. [21]) with the frequencies close enough are used. This is the case we consider below.

Now our task is to determine spatial distributions of $\Omega_s(x)$ and $\Delta_s(x)$ ensuring the condition

$$\nu(x) \equiv n(x) - n^*(x) = 0, \quad (2)$$

where $n(x) = n_r(x) + in_i(x) \approx [1 + \frac{1}{2}\chi_p(x)]\sqrt{\varepsilon_0}$ is the refractive index, for x being either arbitrary or belonging to some interval (see below). $\nu(x)$ will be used to control the accuracy of the obtained \mathcal{PT} -symmetric refractive indexes.

Because of the complexity of the relations among all parameters involved in Eqs. (1), (2), it is not obvious *a priori* that the problem has a solution. Therefore we proceed with analysis of particular systems. To this end we adopt the approach as follows. First, we define a “seed” shape of the susceptibility, of the type we would like to

obtain, say $\chi^{sd}(x, \epsilon_j, \eta)$, which contains a number of free parameters ϵ_j and η . Second, neglecting all terms within some accuracy, say of 10%, from (2) we compute analytical solutions for $\Omega_s^{sd}(x, \epsilon_j, \eta)$ and $\Delta_s^{sd}(x, \epsilon_j, \eta)$. Third we substitute the obtained “seed” Rabi frequencies and Stark shifts in Eq. (1). Due to crude approximations made the so obtained susceptibility may still give significant errors in (2). Our final step is to minimize the error using the control parameters ϵ_j and η .

First, we apply the above algorithm to obtain a \mathcal{PT} -symmetric lattice. Since the main limitation for the lattice period is determined by the Stark field, we require the period to be λ_S , i.e. $\chi(x) = \chi(x + \lambda_S)$. The experimental geometry we bear in mind is illustrated in Fig. 1(b). We further assume that each control field consists two almost parallel plane waves having x -components of the wavevector equal to $k_S = 2\pi/\lambda_S$, i.e. to the Stark field wavevector. Now the seed solution can be chosen as $\chi^{sd} = \epsilon_0 + \epsilon_1 \cos \xi + i\epsilon_2 \sin \xi$, where $\xi = k_S x$ and $\epsilon_{0,1,2}$ are free parameters. As a particular atomic vapor we use a mixture of isotopes ^{87}Rb ($s = 1$) and ^{85}Rb ($s = 2$), and assign $|g, s\rangle = |5S_{1/2}, F = 1\rangle$, $|a, s\rangle = |5S_{1/2}, F = 2\rangle$, and $|e, s\rangle = |5P_{1/2}, F = 1\rangle$ for each specie.

To perform numerical study we further particularize the problem by assuming that $N_1 = 1.26 \times 10^{12} \text{ cm}^{-3}$ and $N_2 = 1.14 \times 10^{12} \text{ cm}^{-3}$ (thus $N = 2.4 \times 10^{12} \text{ cm}^{-3}$). The isotopes are loaded in a cell at approximately 363 K and the coherence decay rates are estimated as $\gamma_{eg} \approx \gamma_{ea} = 2\pi \times 334 \text{ MHz}$ and $\gamma_{ag} = 2\pi \times 16 \text{ kHz}$ [16]. With sufficiently high accuracy we can impose $\alpha_{e,1} - \alpha_{g,1} \approx \alpha_{e,2} - \alpha_{g,2} = 2\pi\hbar \times 0.1223 \text{ Hz}(\text{cm}/\text{V})^2$ and $d_{ae,1} \approx d_{ae,2} = 2.5377 \times 10^{-27} \text{ C}\cdot\text{cm}$ [22], what allows us to consider $\Omega_1 \approx \Omega_2 = \Omega_c$. Other parameters are chosen as $\omega_p \approx \omega_c = 2\pi \times 3.77 \times 10^{14} \text{ s}^{-1}$ ($\lambda_p = 795 \text{ nm}$), $\eta = 0.91$, $\chi_0 = 0.57 s$, $\delta_1 = 1.80\gamma_{eg}$, and $\delta_2 = -0.01\gamma_{eg}$.

As the second step, we solve equation $\chi_p(\Omega_s^{sd}, \Delta_s^{sd}) = \chi^{sd}$ with respect the real Ω_s^{sd} and Δ_s^{sd} . For $|\delta_2| \ll |\delta_1|$ it is possible to leave only the leading terms in δ_2 allowing one to find the solutions explicitly. As the final step, we substitute Ω_s^{sd} and Δ_s^{sd} back into Eq. (1) and obtain $\nu(x)$ as small as possible by tuning the parameters $\epsilon_{0,1,2}$. Since the obtained formulas have rather cumbersome forms they are not presented here. Instead, we write down the final expressions for the control-field Rabi frequency and for the Stark-field amplitude by keeping the first significant harmonics (i.e the terms $\gtrsim 10^{-4}$)

$$\begin{aligned} E_S &= E_0[0.9698 + 0.0053 \cos \xi - 0.0007 \sin \xi], \\ \Omega_c &= \gamma_{eg}[1.5384 + 0.0122 \cos \xi + 0.0232 \sin \xi]. \end{aligned}$$

Here $E_0 = 4 \times 10^5 \text{ V/cm}$ [see Fig. 2(a)]. As we already mentioned, the final shape of the susceptibility differs from the ansatz χ^{sd} . We represent it also in a form of a Fourier series by keeping the first significant harmonics, i.e. $\chi_p(x) = \chi_{0p} + \chi_{1p}(x)$, where $\chi_{0p} \approx 0.2257$ determines

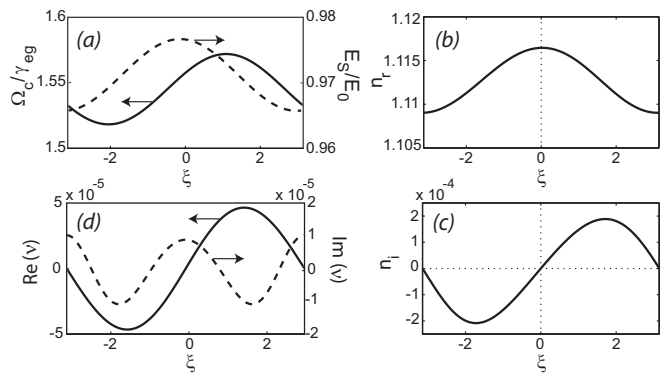


FIG. 2: (a) The Rabi frequency of the control (solid line) and Stark (dashed line) fields vs. ξ . (b) n_r and (c) n_i vs. ξ . (d) Real (solid line) and imaginary (dashed line) parts of the error function $\nu(\xi)$.

the average (in space) refractive index and the periodic part is given by

$$\chi_{1p} \approx 0.0075 \cos \xi + i10^{-4}[3.9418 \sin \xi + 0.2298 \sin(2\xi)]. \quad (3)$$

The real and imaginary parts of the refractive index is respectively shown in Fig. 2(b), (c). We notice that there is a significant difference in the magnitude of the constant real part of the susceptibility and its imaginary part. What is important, however, is that the latter constitutes about several percents of the variation of the real part. In Fig. 2(d) we show errors in obtaining the real and imaginary parts of the susceptibility.

Now turn to the propagation of the probe field along z -direction in the described atomic vapor. Since in the y -direction the medium is homogeneous, in the paraxial approximation the beam propagation is governed by

$$2ik_p \frac{\partial \Omega_p}{\partial z} + \frac{\partial^2 \Omega_p}{\partial x^2} + k_p^2 \chi_{1p}(x) \Omega_p = 0, \quad (4)$$

where $k_p = \omega_p \sqrt{1 + \chi_{0p}}/c$ is the probe-field wavevector. [The beam of constant amplitude in y -direction is chosen only for convenience: one can consider any waveguide structure in y -direction what will result only in the renormalization of the constants in (4)]. By the ansatz $\Omega_p(x, z) = \tilde{\Omega}(x)e^{ibz}$ where b is the propagation constant, we obtain

$$\frac{d^2 \tilde{\Omega}}{d\xi^2} + \frac{k_p^2}{k_S^2} \chi_{1p}(\xi) \tilde{\Omega} = \beta \tilde{\Omega}, \quad \beta = \frac{2k_p}{k_S^2} b. \quad (5)$$

Taking into account the well known results on the periodic potentials [23] as well as rapid decay of the Fourier harmonics in (3), one expects that with high accuracy the spectrum of (5) is indeed pure real. To check this, in Fig. 3(a),(b) we show β obtained numerically for the susceptibility including all terms until the leading term violating the condition (2) (the latter have amplitudes $\lesssim 10^{-5}$).

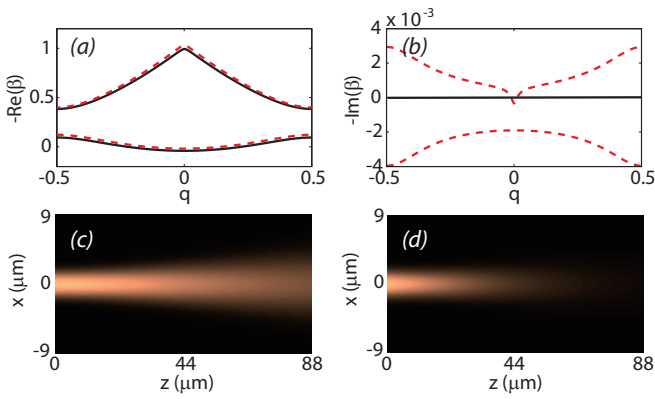


FIG. 3: (Color online) Real (a) and imaginary (b) parts of the dimensionless propagation constant β . Solid (dashed) lines show the results for \mathcal{PT} -symmetric refractive index and non \mathcal{PT} -symmetric refractive index obtained by change of the mutual concentration of species, as explained in the text. Evolution of $|\Omega_p(z)|^2$ in the vapors with \mathcal{PT} -symmetric (c) and non \mathcal{PT} -symmetric (d) refractive indexes.

Let us now clarify whether the described procedure is “structurally stable”, i.e. whether small deviations of system parameters do not break the obtained \mathcal{PT} symmetry. To this end we tested the method with respect to change of mutual concentration of the species. More specifically we have changed the obtained η by 10% and repeated the calculation described by the above algorithm (i.e. we did not use η as a matching parameter any more). We indeed found that now the accuracy with which (2) is satisfied is lower (see Fig. 3(a),(b)) but the imaginary parts are still very small (of order of 10^{-3} [24]). In Fig. 3 we also illustrate propagation for the input Gaussian beam in the discussed \mathcal{PT} -symmetric [panel (c)] and non- \mathcal{PT} -symmetric [panel (d)] structures. The input probe beam $\Omega_p(z=0) = e^{-0.1(k_S x)^2}$ propagates in the \mathcal{PT} -symmetric medium along much longer distance compared to the non \mathcal{PT} -symmetric case where absorption is observed.

The described approach can be used to produce other shapes of the refractive index. As an example we now show how the method can be modified to obtain a \mathcal{PT} symmetric parabolic refractive index [2]. The main idea is based on the fact that \mathcal{PT} -symmetry can be satisfied only locally in space. Then one can “cut” undesirable non- \mathcal{PT} -symmetric distribution of the refractive index by choosing the location of the finite-size vapor cell with respect to the domain where the external field produces local \mathcal{PT} -symmetry. This is illustrated in Fig. 4 (a),(b) where we still consider the mixture of the Rubidium isotopes, but taking now ^{85}Rb as the first, $s=1$, and ^{87}Rb as the second, $s=2$, systems. We choose $N_1 = 2.39 \times 10^{15} \text{ cm}^{-3}$ and $N_2 = 8.98 \times 10^{12} \text{ cm}^{-3}$, $\eta = 0.375 \times 10^{-2}$, $\delta_1 = 3.56 \times 10^{-4} \gamma_{eg}$, and $\delta_2 = 3.93 \times 10^{-3} \gamma_{eg}$, without changing the other parameters. The described procedure

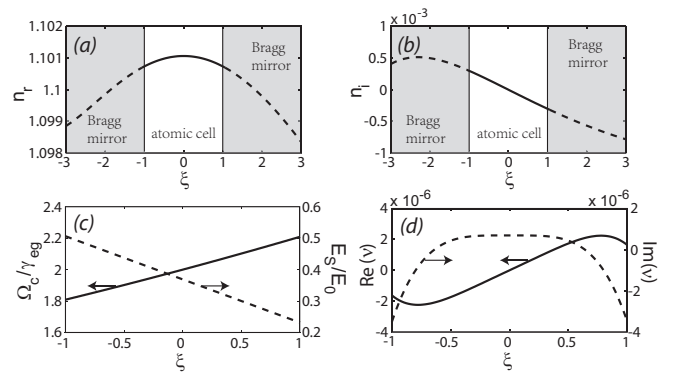


FIG. 4: Real (a) and imaginary (b) parts of the refractive index. Solid line is the refractive index inside the atomic cell limited by Bragg mirrors. Dashed line shows the distribution if the gas would occupy the whole space. (c) Spatial distribution of Stark (dashed line) and control (solid line) fields required for inducing the local \mathcal{PT} -symmetric refractive index. (d) Real (solid line) and imaginary (dashed line) parts of the error function inside the cell.

of the choice of the Stark and control fields is performed to satisfy (2) only locally in space. In particular, this is achieved, by taking $\Omega_c = \gamma_{eg}(2 + 0.2\xi + 0.009\xi^2)$ and $E_S = E_0(0.3695 - 0.1375\xi)$, illustrated in Fig. 4(c). The spatial modulation of the susceptibility now has a complex form [Fig. 4 a, b]. If however the atomic cell (limited say by Bragg mirrors) is situated as shown in the panels, then the atomic vapor changes the refractive index only in the domain occupied by the cell. This domain was chosen to ensure (2) with high accuracy where the real [solid line in panel (a)] and imaginary [solid line in panel (b)] are respectively parabolic and linear. Now the susceptibility inside the atomic cell is described by $\chi_p = 0.2021 - 0.0007\xi^2 - i0.0006\xi$, which obviously satisfies the condition of \mathcal{PT} symmetry.

To conclude, we have suggested a possibility of creating \mathcal{PT} -symmetric profiles of the refractive index in a mixture of resonant atomic gases. An important property of the proposed scheme is the possibility of changing parameters of the structure *in situ*, say by changing wavelengths or amplitudes of the control fields. While we used the well studied isotopes of the Rubidium atoms the proposed scheme allows for further generalization and improvement using other atomic isotopes, four-level atoms, mixtures of more than two isotopes, monoatomic vapors with two control fields, etc. Adding more control parameters opens possibilities of experimental implementation of nonlinear \mathcal{PT} -symmetric susceptibilities [25], as well as combined linear and nonlinear ones [26] which recently attracted much attention.

This work was supported by the Program of Introducing Talents of Discipline to Universities under Grant No. B12024, by NSF-China under Grant Nos. 11174080 and 11105052, as well as by the FCT grants PEST-OE/FIS/UI0618/2011 and PTDC/FIS/112624/2009.

-
- [1] N. N. Bogoliubov, J. Phys. (Moscow) **11**, 23 (1947); P. G. de Gennes, “Superconductivity of Metals and Alloys” (W. A. Benjamin, Inc, New York, 1965).
- [2] T. Kato, *Perturbation theory for linear operators* (Springer-Verlag, 1980).
- [3] C. M. Bender and S. Boettcher, Phys. Rev. Lett. **80**, 5243 (1998).
- [4] C. M. Bender, S. Boettcher, and P. N. Meisinger, J. Math. Phys. **40**, 2201 (1999); C. M. Bender, J. Brod, and M. E. Reuter, J. Phys. A: Math. Gen. **37**, 10139 (2004).
- [5] A. Ruschhaupt, F. Delgado, and J. G. Muga, J. Phys. A: Math. Gen. **38**, L171 (2005).
- [6] C. E. Rüter, K. G. Makris, R. El-Ganainy, D. N. Christodoulides, M. Segev, and D. Kip, Nature Phys. **6**, 192 (2010).
- [7] M. Kulishov, J. M. Laniel, N. Bélanger, J. Azaña, and D. V. Plant Opt. Express **13**, 3068 (2005); Z. Lin, H. Ramezani, T. Eichelkraut, T. Kottos, H. Cao, and D. Christodoulides, Phys. Rev. Lett. **106** 213901 (2011).
- [8] S. Longhi, Phys. Rev. A **82**, 031801 (2010).
- [9] V. V. Konotop, V. S. Shchesnovich, and D. A. Zezyulin, Phys. Lett. A **376**, 2750 (2012).
- [10] H. Benisty, A. Degiron, A. Lupu, A. De Lustrac, S. Chénais, S. Forget, M. Besbes, G. Barbillon, A. Bruyant, S. Blaize, and G. Lérondel, Opt. Express, **19**, 18004 (2011).
- [11] A. Regensburger, C. Bersch, M.-A. Miri, G. Onishchukov, D. N. Christodoulides, and U. Peschel, Nature, **488** 167 (2012).
- [12] M. O. Scully, Phys. Rev. Lett. **67**, 1855 (1991); M. Fleischhauer, C. H. Keitel, M. O. Scully, C. Su, B. T. Ulrich, and S. Y. Zhu, Phys. Rev. A **46**, 1468 (1992).
- [13] A. S. Zibrov, M. D. Lukin, L. Hollberg, D. E. Nikonov, M. O. Scully, H.G. Robinson, and V. L. Velichansky, Phys. Rev. Lett. **76**, 3935 (1996).
- [14] D. D. Yavuz, Phys. Rev. Lett. **95**, 223601 (2005).
- [15] N. A. Proite, B. E. Unks, J. T. Green, and D. D. Yavuz, Phys. Rev. Lett. **101**, 147401 (2008).
- [16] C. O’Brein, P. M. Anisimov, Y. Rostovtsev, and O. Kocharovskaya, Phys. Rev. A **84**, 063835 (2001).
- [17] Z. J. Simmons, N. A. Proite, J. Miles, D. E. Sikes, and D. D. Yavuz, Phys. Rev. A **85**, 053810 (2012).
- [18] see e.g. V. S. Letokhov, *Laser Control of Atoms and Molecules* (Oxford University Press, 2007).
- [19] Y. Bai, S. Slivken, S. R. Darvish, A. Haddadi, B. Gokden, and M. Razeghia, Appl. Phys. Lett. **95**, 221104 (2009).
- [20] Y. Bai, S. R. Darvish, S. Slivken, W. Zhang, A. Evans, J. Nguyen, and M. Razeghi, Appl. Phys. Lett., **92**, 101105 (2008); M. Razeghi, EEE J. Selected Topics in Quantum Electrnics, **15**, 941 (2009).
- [21] J. Gea-Banacloche, Y.-q. Li, S.-z. Jin, and M. Xiao, Phys. Rev. A **51**, 576 (1995)
- [22] D. Steck, ⁸⁷Rb and ⁸⁵Rb D Line Data, <http://steck.us/alkalidata>.
- [23] see e.g. C. M. Bender, G. V. Dunne, and P. N. Meisinger, Phys. Lett. A, **252**, 272 (1999); J. K. Boyd, J. Math. Phys. **42**, 15 (2001); J. M. Cerveró and A. Rodríguez, J. Phys. A: Math. Gen. **37**, 10167 (2004); K. G. Makris, R. El-Ganainy, D. N. Christodoulides, and Z. H. Musslimani Phys. Rev. Lett. **100**, 103904 (2008); B. Midya, B. Roy, and R. Roychoudhury, Phys. Lett. A **374**, 2605 (2010).
- [24] Here the complex propagation constant is related to violation of (2) rather than to the \mathcal{PT} -symmetry breaking. With the accuracy 10^{-4} the optimized susceptibility has the form $\chi_p = 0.2298 + 0.0076 \cos \xi + i[0.0026 + 10^{-4}(4.0083 \sin \xi + 1.8217 \cos \xi)]$, i.e. its constant part results in the absorption of the light.
- [25] F. Kh. Abdullaev, Y. V. Kartashov, V. V. Konotop, and D. A. Zezyulin, Phys. Rev. A **83**, 041805(R) (2011); D. A. Zezyulin, Y. V. Kartashov, V. V. Konotop, Europhys. Lett. **96**, 64003 (2011).
- [26] S. Nixon, L. Ge, and J. Yang, Phys. Rev. A **85**, 023822 (2012); Y. He, X. Zhu, D. Mihalache, J. Liu, and Z. Chen, Phys. Rev. A, **85**, 013831 (2012)